PHYSICAL REVIEW B VOLUME 47, NUMBER 20 15 MAY 1993-II

First-principles study of potassium adsorption on graphite

Francesco Ancilotto
Dipartimento di Fisica "G. Galilei," Università di Padova, via Marzolo 8, I-35131 Padova, Italy

Flavio Toigo
Dipartimento di Fisica "G. Galilei," Universitá di Padova, via Marzolo 8, I-35131 Padova, Italy
and Department of Physics, Pennsylvania State University, University Park, Pennsylvania 16802

(Received 2 October 1992; revised manuscript received 2 December 1992)

Theoretical results obtained with first-principles total-energy calculations are reported for potassium adsorption on the graphite (0001) surface. The structural parameters, the chemisorption energies, and the electronic properties of the K-graphite system are studied at two representative coverages, i.e., in the triangular (2×2) overlayer phase and at a lower coverage. The K-graphite bonding is characterized by a partial charge transfer from the adatom towards the substrate in the low-coverage regime, while in the (2×2) phase a lower charge transfer is accompanied by a redistribution of the electronic charge within the K overlayer. A very smooth surface characterizes the (2×2) K overlayer, which may help in explaining the exceedingly small diffracted intensities of He atoms from K-covered graphite recently reported. The unusual vibrational properties of the (2×2) overlayer are also studied and compared with recent experimental results.

I. INTRODUCTION

Studies of alkali-metal adsorption on solid surfaces have been reported over the last decade and have played an important role in the development of theories of chemisorption.[1] Due to the relative simplicity of their electronic structure the alkali metals are ideal candidates to study the fundamental aspects of adatom-surface chemisorption interactions. Despite the amount of experimental and theoretical work over the years, however, the nature of the alkali-atom–surface interaction is still the subject of current debate. Even in the apparently simple case of alkali metals adsorbed on unreconstructed metal surfaces, fundamental questions regarding the nature (ionic versus covalent) of bonding, the preferred adsorption sites, and the structural details of the resulting ordered overlayers are a matter of controversy.[2]

Among the various substrates which can be used in adsorption studies, exfoliated graphite represents an ideal one because it provides a large-area adsorption surface which is chemically inert, almost defect-free, and very homogeneous. In recent years, a number of experimental and theoretical studies have been reported on alkali metals adsorbed on the graphites (0001) surface.[3–8] In spite of the similarities in the chemical bonding properties of the alkali metals in the bulk phase, rather different behaviors are found experimentally when they are adsorbed on the graphite surface. Lithium exposure results in a hcp incommensurate superstructure. Depending on temperature and coverage conditions, cesium can either form intercalation compounds or be adsorbed in a (2×2) or incommensurate hexagonal.[6] Sodium, on the other hand, does not show any ordered overlayer pattern when adsorbed on the graphite (0001) surface. Potassium, when evaporated onto a high-step-density surface, results in intercalation into the graphite. When it adsorbs on a low-defect surface instead, an ordered (2×2) phase is formed[9] which corresponds to a triangular overlayer where the spacing between K adatoms is $2a_0$ (a_0 being the graphite surface lattice parameter), i.e., $\sim 8\%$ larger than in the bcc bulk phase. Further adsorption of potassium results in the formation of a $(\sqrt{3}\times\sqrt{3})R\,30^\circ$ overlayer structure.[9]

Very recently, an unusual structural phase transition on K-graphite has been reported.[5] At very low K coverage, a dispersed phase with a giant K-K distance (~ 60 Å) is observed. Upon exposure to additional K atoms, this phase is gradually compressed up to a critical coverage where the (2×2) phase starts to grow until the whole surface is covered by it. According to the experimental results of Ref. 5, the bonding of K atoms in the very low-coverage regime is characterized by a relatively large charge transfer ($\sim 0.7e$) from the K atoms to the graphite substrate, while the charge transfer towards the substrate decreases as the coverage increases. When the (2×2) phase is finally formed, the charge redistribution is mainly confined within the K adlayer, which behaves as a quasi-dimensional metal. Theoretical calculations,[10] based on semiempirical tight-binding methods, give support to the above picture, whereas earlier experimental results[7] suggest that even at adatom densities where the (2×2) phase is formed, the K atoms transfer almost completely their valence electrons to the graphite substrate.

Alkali-metal-plated graphite has been proposed[11] as a convenient substrate for studying the two-dimensional behavior of normal and superfluid He films because both the interaction strength and the corrugation of the He-surface potential are expected to be very weak, as has been confirmed recently by He scattering experiments on (2×2) alkali overlayers on graphite.[4] However, although the corrugations in the He-surface potential resulting from the theoretical calculations of Ref. 4 are rather small, the experiments indicate that these surfaces are even less corrugated, the experimental ratio of diffracted-to-specular intensity being <0.001, whereas the predicted one is ~ 0.05.

Another set of intriguing experimental results concerns the vibrational properties of (2×2) overlayers of alkali metals on graphite.[3] The data reported in Ref. 3, based on inelastic He atom scattering experiments, show the presence of very low-energy vibrational modes of the overlayers (ranging from 2.3 meV for Cs to 4.4 meV for K), which are nearly flat away from the zone center and whose microscopic nature has not yet been identified.

In the attempt to clarify the above issues and to provide additional insight towards the understanding of the alkali-graphite interaction, we have carried out first-principles pseudopotential calculations of potassium adsorption on the graphite (0001) surface at two representative coverages: one corresponding to the observed (2×2) overlayer structure (i.e., 1 K atom every 4 graphite surface unit cells) and the second at a lower coverage, corresponding to an ordered phase with a surface density of 1 K atom every 16 graphite unit cells. In the following section we give a brief description of the method used in our calculations. Our results for the structural, electronic, and vibrational properties of the K-graphite system at the two coverages are presented in Sec. III. A summary is given in Sec. IV.

II. COMPUTATIONAL METHOD

The calculations of carbon properties within first-principles pseudopotential methods are computationally very demanding due to the large number of basis functions usually needed to describe appropriately its electronic wave functions.[12,13] For this reason we decided to model the graphite substrate in our calculations with a single, isolated graphite monolayer. This drastic approximation, which has been used in other theoretical calculations of atom chemisorption on graphite,[10,14] is to some extent justified by the anisotropic character of bonding in graphite where the coupling between adjacent graphite layers is much weaker than the in-plane coupling between carbon atoms. This implies that the electronic properties of an isolated monolayer can often provide a reasonable picture of the electronic properties of the infinite crystal.[15]

Our calculations are based on the density-functional (DF) formalism and *ab initio* atomic pseudopotentials. We have used a periodically repeated supercell containing a graphite monolayer of 32 carbon atoms plus K adatoms to model the K-graphite system. A vacuum region ~ 22 a.u. wide is used to decouple the graphite-adsorbate system from its repeated images.[16] The geometry used is shown in Fig. 1, where four K atoms in an ideal (2×2) overlayer over the graphite monolayer are shown. The valence electrons are treated in the local-density approximation (LDA) of DF theory, with the Ceperley-Alder-Perdew-Zunger expression for the correlation functional.[17]

The interaction between carbon ion cores and valence electrons is described by a nonlocal *ab initio* pseudopotential[18] in the Kleinman-Bylander separable form.[19] Only the $l=0$ nonlocality is explicitly used for carbon. A local pseudopotential, derived by accurate *ab initio* pseudopotentials,[20] is used for potassium. This pseudopotential was derived by including the nonlinear core correction in the exchange-correlation functional.[21] The standard linear approximation in the exchange-correlation functional which is generally adopted in LDA-DF calculations is known to give a contraction of the atomic size for the alkali metals, due to a significant overlap between the p-type core orbitals with the s-type valence orbitals. In order to predict the correct bond distances for the alkali metals in pseudopotential calculations, it is necessary to correct the above functional through the nonlinear core correction.

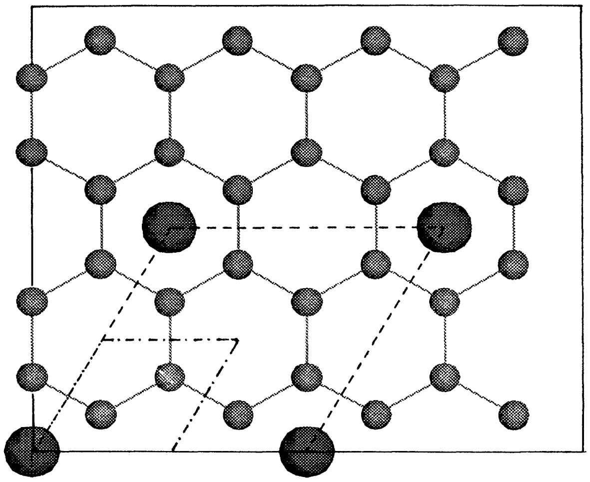

FIG. 1. Top view of the surface supercell geometry used in the present calculations. The small balls represent C atoms, the bigger ones K atoms. The latter are arranged in a (2×2) phase with one K atom, sitting on a hollow site, every four graphite conventional unit cells (this phase corresponds to a coverage $\Theta=\frac{1}{4}$ according to the convention used in the text). The dashed lines show the (2×2) unit cell, the dash-dotted lines the conventional unit cell of two-dimensional graphite.

Only the Kohn-Sham orbitals at the Γ point in the Brillouin zone (BZ) of our supercell are used and expanded in plane waves with a kinetic energy cutoff of 35 Ry, corresponding to $\sim 28\,000$ plane waves. Such a high number of basis functions is required in order to give a sufficiently accurate description of the complex bonding properties of carbon systems.[13]

The above approximations (basis set size, pseudopotentials, and cell size) have been extensively tested for carbon in different bonding environments and compared to experimental and theoretical LDA all-electron results.[13] As a test of the accuracy of the above approximations for potassium, we have calculated the equilibrium distance d_{eq} and the vibrational frequency ω_v of the dimer K_2. We find $d_{\mathrm{eq}}=7.18$ a.u. and $\omega_v=11.9$ meV, i.e., $\sim 4\%$ smaller and $\sim 3\%$ larger than the corresponding experimental values,[22] respectively.

The optimum lattice parameter a_0 of the clean graphite monolayer has been searched by performing a number of total-energy calculations for different values of a_0. The value which minimizes the total energy of the monolayer turns out to be $a_0=4.67$ a.u., in agreement with the results of accurate all-electron calculations[23] and close to the experimental value $a_0=4.651$ a.u. for bulk graphite (throughout the paper, lengths are given in units of the Bohr radius).

We performed our calculations of K-graphite adsorption at two different coverages Θ (Θ is defined as the ratio of the number of alkali adatoms to the number of graphite surface unit cells), i.e., $\Theta=\frac{1}{4}$, corresponding to the adatom density in the (2×2) overlayer structure shown in Fig. 1, and $\Theta=\frac{1}{16}$, corresponding to a more sparse (ordered) phase where only one K atom is retained in the supercell shown in Fig. 1.

At each coverage Θ we carried out two kinds of total-energy calculations, where the C atoms in the graphite monolayer are either kept fixed in their ideal equilibrium positions or they are allowed to relax towards new equilibrium positions. In the unrelaxed-substrate calculations, however, we always optimize the vertical position of the K adatoms with respect to the graphite surface in order to obtain a minimum-energy equilibrium configuration.

The relaxation of the graphite layer in the presence of K adatoms, when allowed, is efficiently performed by using the Car-Parrinello (CP) method.[24] The combined minimization of the CP energy functional with respect to the electronic and ionic degrees of freedom, which allows one to find minimum-energy atomic configurations, is performed in our calculations by using an efficient mixed algorithm combining a quenched-molecular dynamics with a fictitious steepest-descent dynamics.

III. RESULTS AND DISCUSSION

We investigated two sites on the graphite monolayer as possible adsorption sites for a K atom, i.e., the threefold-hollow site at the center of a carbon hexagon and the top site directly above a C atom. Whereas noble gases on graphite are known to adsorb preferably on hollow sites, the top site is the energetically favored site in the case of Al adsorption.[25]

We find that both sites are stable adsorption sites for potassium. However, the results of a partial optimization (i.e., with the C atoms fixed) show that the K adatom prefers the hollow site to the topsite, the difference in binding energies between the two sites being ~0.08 eV. Experimental information on the adsorption sites of alkali on graphite is only available for Cs-(2×2), where low-energy electron-diffraction (LEED) data show that the Cs atom is adsorbed on the hollow site, ~5.3 a.u. above the graphite surface, and that graphite remains essentially in its bulk structure.[26]

In Table I we report our results for the K-graphite equilibrium distances and binding energies. The latter is defined as $E_b^{(\text{K-C})}=-(1/N_{\text{K}})(E_{\text{K-C}}-E_{\text{K}}-E_{\text{C}})$, where $E_{\text{K-C}}$ is the total energy of the K-graphite system, E_{K} (E_{C}) is the total energy of the isolated K (C) monolayer, with atoms in their equilibrium positions, and N_{K} is the number of K adatoms in the supercell. We report the values for the unrelaxed graphite substrate and (in parentheses) those calculated when the graphite monolayer is allowed to relax.

Only the experimental value for the K-graphite equilibrium distance in the (2×2) phase is available, $d_{\text{eq}}\sim 5.1$ a.u.,[27] which is in reasonable agreement with the values $d_{\text{eq}}\sim 5.33-5.36$ a.u. reported in Table I. An additional energy per adatom $E_b^{(\text{K})}=-\frac{1}{4}E_{\text{K}}+E_{\text{K}}^{\text{at}}\sim 0.56$ eV is gained from the binding of K atoms in the isolated (2×2) monolayer.[28]

It appears from Table I that in the low-coverage phase the K adatom is more tightly bound to the substrate than in the (2×2) phase. This is consistent with the experimental results of Ref. 3, where the K-graphite vibrational frequencies, as measured by inelastic He scattering, are found to be higher in the low-coverage regime than in the (2×2) overlayer phase.

The very large energy gain reported in Table I for the (2×2) structure after the relaxation of the graphite substrate is largely due to the development of out-of-plane distortions of the graphite monolayer from its ideal structure. The pattern of displacements in the low-coverage case, $\Theta=\frac{1}{16}$, is characterized by a vertical depression $\Delta z\sim -0.1$ a.u. of the C atoms in the hexagon occupied by the K adatom, while distortions of the same magnitude develop all over the graphite monolayer at the coverage $\Theta=\frac{1}{4}$. In the latter case the C atoms are sensibly buckled along the vertical direction after relaxation, although the pattern of distortions shows no definite symmetry.

Nonplanarity of the graphite surface atoms upon adsorption of Al atoms has been found in the theoretical finite-cluster calculations of Ref. 14. In that case it is shown that small out-of-plane distortions favor the on-top chemisorption of Al since the local environment of C atoms changes slightly from sp^2 to sp^3 type and the vacant electron, which in a planar surface is delocalized, localizes in the hybrid at the fourth vacant coordination site, becoming available for binding the Al adatom. In the present case, however, such a mechanism should not be effective, since adsorption takes place at hollow sites rather than on top sites.

Although an adatom-induced reconstruction of the graphite substrate cannot be excluded in the present case, the distortions that we find are probably affected by the approximations used in our calculations. First, the displacements of C atoms from their ideal positions in the surface layer are expected to be magnified in our monolayer calculations by the absence of the underlying bulk structure.

Moreover, due to our choice of the supercell geometry,

TABLE I. Calculated K-graphite equilibrium distances and binding energies (per K atom) at the two coverages investigated. In parentheses we report the corresponding quantities when the graphite monolayer is allowed to relax in the presence of the K adatoms. Distances are in a.u. and energies in eV.

Θ	d_{eq}	E_b
$\frac{1}{16}$	5.23 (5.15)	0.78 (0.89)
$\frac{1}{4}$	5.33 (5.36)	0.48 (0.76)

the set of **k** points of the surface BZ of graphite which are folded at the point $\overline{\Gamma}$ of our supercell does not include the $\overline{K}$ point at the BZ corner, where the Fermi level crosses the π bands in real graphite. A finite, even if small, energy gap thus separates the occupied states from the empty states of the clean monolayer, making it a semiconductor. Although this has a very small effect on the properties of the ideal monolayer, as it turns out from our calculations, when relaxation is allowed it could favor a spontaneous $sp^2 \rightarrow sp^3$ buckling distortion of C atoms typical of semiconducting carbon.

We cannot distinguish, at this stage, to what extent the distortions found are an artifact of our slab calculations. More converged calculations (with respect to the size of the cell, i.e., to the number of **k** points used in BZ summations) are required in order to give a quantitative answer to the important question of whether reconstruction of the graphite surface takes place in the presence of adsorbates. In the following we will quote separately our results for the unrelaxed and relaxed substrates. Those for the relaxed substrate (included the values reported in Table I in parentheses), should be taken with caution, for the reasons described above.

In order to study the charge redistribution accompanying the K-graphite bond formation, we computed the difference charge density $\Delta\rho(\mathbf{r})=\rho_{\text{K-C}}-(\rho_{\text{K}}+\rho_{\text{C}})$ calculated by taking as reference the superposition of the electronic charge densities of the clean graphite monolayer, $\rho_{\text{C}}(\mathbf{r})$, and that of the isolated K monolayer, $\rho_{\text{K}}(\mathbf{r})$, with the C and K atoms in their equilibrium positions. In Fig. 2 we show the projection of $\Delta\rho(\mathbf{r})$ onto a plane normal to the surface plane and parallel to the vertical axis in Fig. 1. It appears from Fig. 2(a), which refers to the low-coverage case with one K atom in our supercell, that charge is removed both from the 4s orbital of potassium and from the C-C σ bonds of the graphite layer, and transferred mainly to the interface region between the K atom and graphite. As shown in the following, the charge transferred towards the graphite plane actually fills the available π^* antibonding orbitals of clean graphite.

In Fig. 2(b) a similar pattern of charge redistribution is observed in the case of the (2×2) overlayer. Here charge is depleted both from the interstitial regions between K atoms in the metallic overlayer and from the carbon layer. Note that for $\Theta=\frac{1}{16}$ [Fig. 2(a)], despite the very large distance between the K adatom and its repeated images [$d_{\text{K-K}}\sim16$ a.u. along the horizontal axis in Fig. 2(a)], a non-negligible amount of charge piles up in the region between the adatoms. This is a consequence of the delocalized character of the K valence electron when it is partially donated to the graphite substrate, as will be shown in the following.

An estimate of the charge transferred from the K adatoms to the graphite surface can be obtained by averaging $\Delta\rho(\mathbf{r})$ on planes parallel to the surface, $\overline{\Delta\rho}(z)=(1/N_{\text{K}})\int dx \int dy\, \Delta\rho(\mathbf{r})$. The results of such an average are shown in Fig. 3. In each panel we show $\overline{\Delta\rho}(z)$ for the unrelaxed and the relaxed substrate, with solid and dashed lines, respectively. Note that the differences in the two cases are minor, and this is especially true for the (2×2) overlayer [Fig. 3(b)]. If we define the charge transferred from the potassium layer to graphite, ΔQ, as the area underlying the negative peaks

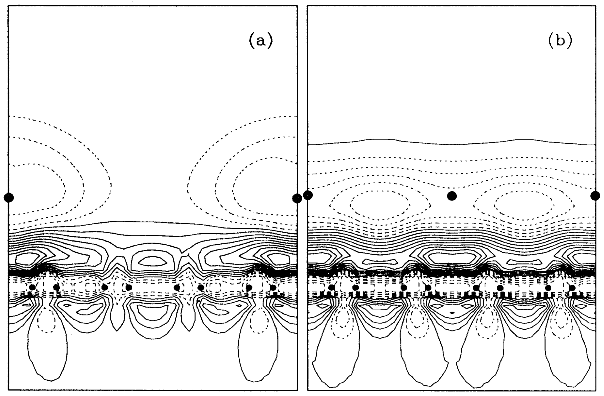

FIG. 2. Difference charge density $\Delta\rho=\rho_{\text{K-C}}-(\rho_{\text{K}}+\rho_{\text{C}})$ projected onto a plane perpendicular to the surface layer and parallel to the vertical axis in Fig. 1. The small (big) dots show the projected positions of carbon (potassium) atoms. (a) $\Theta=\frac{1}{16}$; (b) $\Theta=\frac{1}{4}$. Dashed (solid) lines indicate negative (positive) values of $\Delta\rho$, respectively.

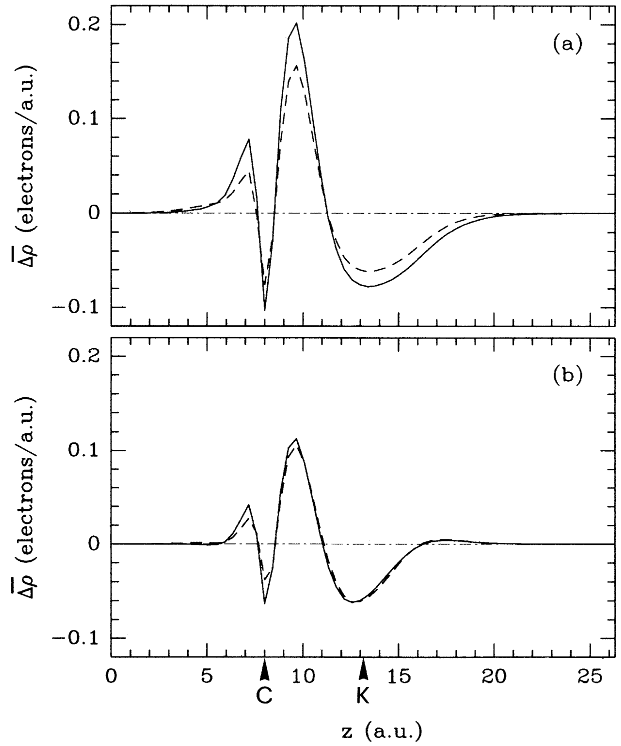

FIG. 3. Lateral average $\overline{\Delta\rho}(z)$ of the difference charge density $\rho_{\text{K-C}}-(\rho_{\text{K}}+\rho_{\text{C}})$ plotted as a function of the vertical distance. The position of the graphite monolayer and of the K adatoms are shown by arrows. (a) $\Theta=\frac{1}{16}$; (b) $\Theta=\frac{1}{4}$. The solid (dashed) lines show the result for the unrelaxed (relaxed) graphite monolayer, respectively.

centered at the K position in Figs. 3(a) and 3(b), we find $\Delta Q=0.38e$ and $\Delta Q=0.18e$ for $\Theta=\frac{1}{16}$ and $\Theta=\frac{1}{4}$, respectively, in the case of the unrelaxed substrate. If the relaxation of the graphite surface is allowed, these values change to $\Delta Q=0.28e$ and $\Delta Q=0.17e$, respectively. The above values are in qualitative agreement with the theoretical results of Ref. 10, based on semiempirical tight-binding calculations, where the values $\Delta Q=0.40e$ and $\Delta Q=0.13e$ are reported for the corresponding surface densities of K adatoms.

Experiments seems to indicate[5] that at very low K coverage ($\Theta \ll \frac{1}{40}$ in our notation) the charge transfer towards the substrate is $\sim 0.7e$, remaining largely constant in the low-density regime, while it decreases as the surface density of K adatoms increases, becoming much smaller in the (2×2) phase, where the charge redistribution takes place mainly within the (2×2) potassium monolayer. Our results are in agreement with the above picture, whereas they disagree with earlier experimental results,[7] indicating a complete charge transfer of the alkali s electron to the π^* conduction-band states even in the high-coverage (2×2) phase.

We next analyze the nature of the single-electron Kohn-Sham states involved in the K-graphite bond formation. In Fig. 4 we show the calculated energy position of the highest occupied electronic states close to the top of the valence band of the graphite monolayer, for the two coverages investigated. In each of the two panels we show the level positions for the unrelaxed (b) and the relaxed (c) graphite substrate. For comparison, the energy levels for the noninteracting system (i.e., isolated K and graphite monolayers) are also shown with dashed lines in the left part of the two panels.

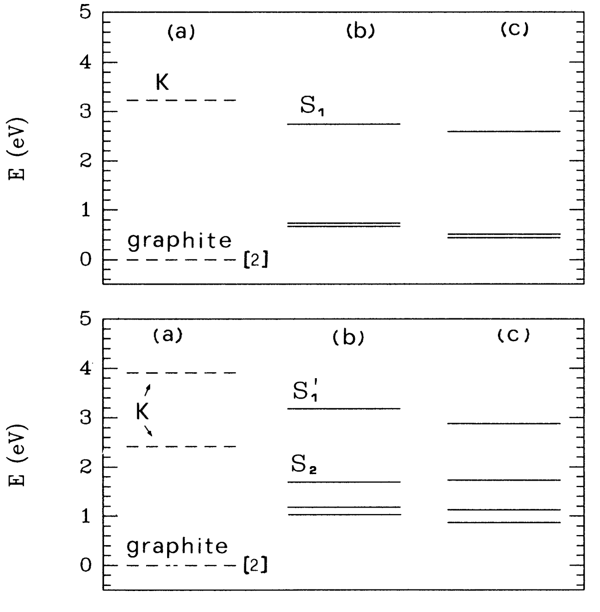

FIG. 4. Energy diagram of the electronic states introduced by the K adatoms. Upper panel: $\Theta=\frac{1}{16}$. Lower panel: $\Theta=\frac{1}{4}$. The dashed lines (a) show the energy levels of the noninteracting system (i.e., isolated K and graphite monolayers). The zero of energy is taken at the highest (twofold degenerate) occupied state in the clean graphite monolayer. In both panels, (b) refers to the case of unrelaxed substrate and (c) to the case of relaxed substrate.

In the low-coverage case (upper panel in Fig. 4), a state associated with the K adatom (labeled S_1) appears ~ 2 eV above the highest occupied state of the graphite monolayer. A contour plot of the charge density in this state is shown in Fig. 5(a). It appears that the charge from the K adatoms is transferred into one of the lowest unoccupied π^* states of the clean graphite monolayer. Figure 5(a) shows that the state S_1 is quite delocalized across the surface, i.e., a fraction of the charge is transferred also to the p_z-like orbitals located on more distant C atoms. This delocalized character accounts for the non-negligible charge overlap between nearest-neighbors K atoms appearing in Fig. 2(a).

In the case of the (2×2) overlayer (lower panel in Fig. 4), besides the state S_1', whose nature is very similar to that of the state S_1 of the low-coverage phase, an additional (doubly occupied) state (labeled S_2 in Fig. 4) appears close to the valence-band edge of the graphite monolayer. A contour plot of the charge density in the state S_2 is shown in Fig. 5(b). The electrons in this state appear to be quite delocalized within the K monolayer, as expected for a metallic system. The similarities of Fig. 5(b) with the charge density of an isolated (2×2) K monolayer could suggest that the state S_2 arises mainly from the K $4s$ electrons. We remark, however, that a definite statement about the exact character of this state would require a more systematic analysis of other competing states, i.e., the K $3d$,C $2p_z$, and the C-interlayer state found in alkali-metal graphite intercalation compounds.[29] In these compounds the strongly dispersed state whose charge is confined within the alkali layer, rather than arising from the alkali s-electron states, is actually an interlayer quasi-free-electron state which preexists in the clean monolayer graphite at ~ 5 eV above the Fermi level.

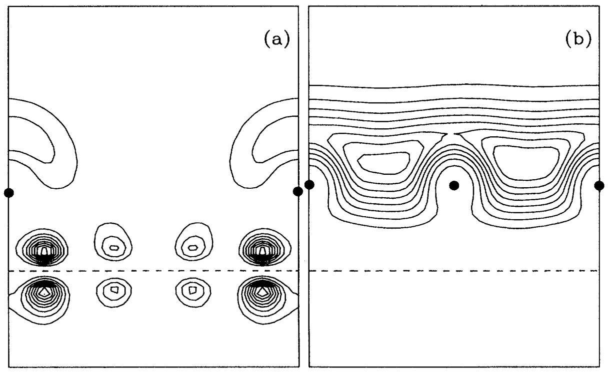

FIG. 5. Contour plot of the valence charge densities for the two states labeled S_1 and S_2 in Fig. 4, in a plane perpendicular to the surface and passing through the lower row of K atoms shown in Fig. 1. Both plots refer to the case of an ideal graphite substrate. The dots show the position of the K adatoms, while a dashed line indicates where the graphite monolayer is located.

Figure 5(b) suggests that the surface corrugation of the (2×2) overlayer should be rather small. In the upper panel of Fig. 6 we show a contour plot of the calculated total valence electron charge density above the (2×2) K overlayer. The main feature appearing in Fig. 6(a) is the very small corrugations of the surface of constant charge density at large distances.

A smooth surface implies a smooth repulsive potential as experienced, e.g., by a He atom at thermal energies approaching the K-plated graphite in a scattering experiment like the one described in Refs. 3 and 4. In an effective-medium theory[30] the He-surface repulsive potential is directly proportional to the unperturbed electronic charge density, $V^{\mathrm{rep}}=\alpha\rho(\mathbf{r})$, where α depends only weakly on the nature of the surface. Within such theory, the diffraction of scattered atoms directly probes the surface electronic structure and thus the surface geometry.

The recent experimental results reported in Ref. 4 for He scattering from (2×2) alkali overlayers on graphite have shown an exceedingly small corrugation of the He-surface potential. Theoretical calculations,[4] based on the ansatz $V^{\mathrm{rep}}=\alpha\rho(\mathbf{r})$, and where the valence charge density of the alkali overlayer is modeled by a superposition of atomic charge densities, $\rho_v^{(\mathrm{at})}$, predict a rather small ratio of the diffracted-to-specular intensity, ∼0.05 for He atoms scattered by a (2×2) potassium overlayer. A contour plot of the electronic charge density $\rho_v^{(\mathrm{at})}$ used in the calculations of Ref. 4 is shown in Fig. 6(b). No He diffraction is actually observed in the experiments,[4] indicating that the corrugation of the He-surface potential is even smaller than predicted. This null result together with the resolution of the experimental apparatus allows one to only place an experimental upper limit to the above ratio, ∼0.001.[4]

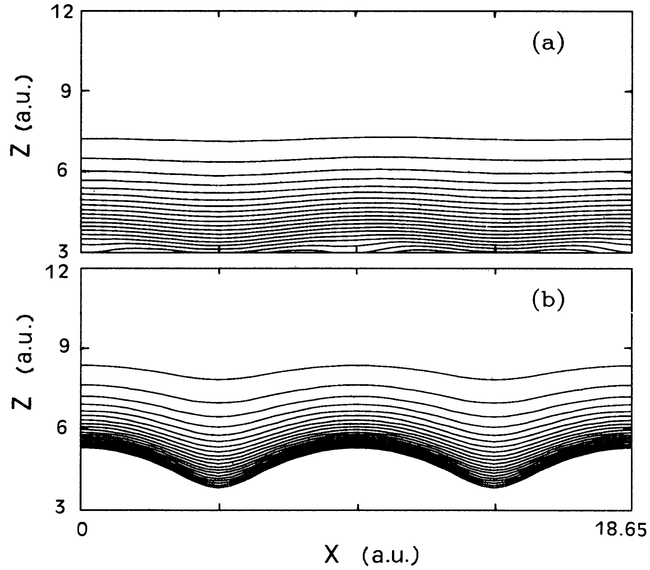

FIG. 6. Contour plot of the valence charge densities above the (2×2) overlayer of potassium, in the same vertical plane of Fig. 5. The distance z is calculated from the position of the K adlayer. In (a) the self-consistent charge density from our calculations is shown, while (b) shows the electron charge density of a (2×2) K overlayer as obtained from a superposition of individual atomic charge densities. The functional form $\phi_0\exp(-kr)/(kr)$, with $k=0.83$ a.u. and $\phi_0=0.36$ a.u. has been used to fit the long-range tail of the atomic charge density of potassium (Ref. 4). The outermost contour in both panels is drawn at $\rho=5\times10^{-5}$ a.u.$^{-3}$ and consecutive levels are separated by $\Delta\rho=5\times10^{-5}$ a.u.$^{-3}$.

The outermost contour in Figs. 6(a) and 6(b) is drawn at $\rho=5\times10^{-5}$ a.u.$^{-3}$, i.e., it coincides with the locus of classical turning points of a He atom of energy 17.5 meV if one takes $\alpha\sim350$ eV a.u.^{3} (Ref. 31) (for the purpose of comparison, we choose the experimental value of Ref. 4 as the energy of the incident He atom). From the charge-density corrugation profile we find that the Fourier component V_G^{rep} relative to the six smallest G vectors of the (2×2) surface BZ, which gives the dominant contribution to the corrugation of V^{rep} in the case of a rather smooth surface, is $\sim\frac{1}{4}$ of that computed by using the superposition of atomic charge densities shown in Fig. 6(b). Since the diffracted intensities of the He beam are roughly proportional to $|V_G^{\mathrm{rep}}|^2$, more than an order of magnitude reduction in the calculated intensities is expected by using the self-consistent charge density instead of $\rho_v^{(\mathrm{at})}$, in qualitative agreement with the experimental results of Ref. 4. A more quantitative comparison with He diffraction experimental data requires in addition the knowledge of the van der Waals attractive part of the He-surface potential, and is out of the scope of the present calculations.

The validity of the assumption $V^{\mathrm{rep}}=\alpha\rho(\mathbf{r})$, where a superposition of atomic charge densities is used to model $\rho(\mathbf{r})$, has been verified for a number of surfaces including Cu(110), Ag(110), Au(110), Ni(100), and Ti(0001).[32–35] In particular, the superposition of atomic charge densities is found to be almost indistinguishable, in the low-density region important for He scattering, from the charge density as obtained from *ab initio*, all-electron calculations. Note that the above approximation is found to work for relatively uncorrugated surfaces such as Ni(100) as well as for highly corrugated, reconstructed surfaces such as Au(110). Our results represent a counter-example where the use of superpositions of atomic charge densities can lead to incorrect results. In the present case, the reduction of the corrugation is the consequence of the combined effect of charge transfer to the substrate and of redistribution of charge within the K monolayer.

As a final remark, we note that the self-consistent charge density as calculated within pseudopotential-LDA methods is known to have an exponential decay in the low-density region which is faster than that computed with other *ab initio* methods such as, e.g., the all-electron (LDA) full-potential linearized augmented plane-wave method.[36] The latter scheme should be preferred to the pseudopotential-LDA method if a very accurate determination of the charge density far from the surface is needed.

The vibrational properties of alkali monolayers adsorbed on graphite have been the subject of a recent experimental study,[3] where inelastic He atom scattering has revealed very low-energy, nearly dispersionless modes of the (2×2) overlayer of K, Rb, and Cs adsorbed on graphite (0001). Almost flat phonon modes at 4.4 and 6.5 meV have been observed for K in the (2×2) phase and in a more disperse phase, respectively, which have been tentatively attributed[3] to vibrations of the alkali atoms in a plane perpendicular to the graphite surface.

Such assignment implies that the force constants of the alkali-graphite bonds are rather small, even smaller than those between physisorbed rare-gas atoms and graphite (even if the binding energies of alkali metals on graphite are much higher than those of rare gases). However, the results of neutron scattering experiments[37] on the graphite intercalation compound (GIC) KC_8, where the K ordering between graphite layers is (2×2), indicate that the force constants between alkali and carbon layers are much larger than those between carbon layers in pure graphite. Since the zone-center optical mode polarized along the [001] direction is found in pure graphite at ~ 16 meV,[38,39] it seems unlikely that a similarly polarized mode for the K (2×2) overlayer should be found at ~ 4 meV only.

If one uses a simple one-dimensional mass-and-spring model to fit the experimental dispersion of the longitudinal modes of KC_8 along the [001] direction as measured in Ref. 37, one finds a force constant $\kappa_{\text{K-C}} \sim 0.021$ a.u. for relative displacements of the alkali and carbon layers, to be compared with the force constant between adjacent carbon layers in pure graphite for displacements along the same directions, $\kappa_{\text{C}} \sim 0.0018$ a.u. We notice that in KC_8 the ordering of K atoms is the same as in the present case. Moreover, upon intercalation of K, the distance between adjacent graphite planes increases considerably, from 6.33 a.u. for pure graphite to ~ 10.4 a.u.,[9] i.e., the K-graphite distance $d_{\text{K-C}} \sim 5.2$ a.u. in KC_8 is very close to the value we find for the equilibrium distance of the (2×2) overlayer. Thus we expect that the force constant $\kappa_{\text{K-C}}$ should not be much different from that of the (2×2) K-graphite system.

As an order-of-magnitude estimate for the vibrational frequency of the overlayer at the *BZ* center, we may take $\omega = (\kappa_{\text{K-C}}/M_{\text{K}})^{1/2}$, M_{K} being the mass of a K atom. This gives $\omega \sim 15$ meV, i.e., a much larger frequency than the experimental value $\omega \sim 4.4$ meV measured in Ref. 3. This suggests the hypothesis that the low-energy mode observed using He scattering is not a mode polarized normal to the surface.

In the attempt to substantiate this hypothesis, we performed a number of static calculations for our (2×2) geometry intended to simulate "frozen" phonon modes of the K overlayer. In these calculations only the K atoms are displaced from their equilibrium positions, while the C atoms in the graphite monolayer are kept in their ideal positions. The resulting variations in the total energy with respect to the equilibrium configuration are interpolated by using quadratic forms, in order to extract force constants κ.

We first investigated the modes at the $\overline{\Gamma}$ and $\overline{M}$ points of the overlayer surface BZ, where the K atom displacements from equilibrium are perpendicular to the surface. Again, we simply take $\omega = (\kappa/M_{\text{K}})^{1/2}$, i.e., we consider the K overlayer mode as completely decoupled from the collective vibrational modes of the graphite substrate.

As expected, the resulting frequencies are much larger than those measured experimentally. We thus tried a different displacement pattern, namely in-plane "bond-bending" displacements of the K adatoms, again at the $\overline{\Gamma}$ and $\overline{M}$ points, and find frequencies in the range 4–6 meV, i.e., close to the experimental values of Ref. 3.

We summarize our results in Fig. 7, where the calculated frequencies of the modes described above are compared to the results of Ref. 3. Note that the dispersive part of the experimental phonon curve at low wave vectors arises from hybridization of the overlayer vibrations with the graphite surface Rayleigh mode, which is expected in the same range of energy and wave vectors.

The effect of including the mixing of the K overlayer modes with those of the graphite substrate, which is neglected in our simple frequency estimates, should be large close to $\overline{\Gamma}$, where the modes Γ_1 and Γ_2 in Fig. 7 are degenerate in energy with the band of low-energy graphite surface modes.[40] However, away from the zone center, where no graphite modes are present in the energy range of Fig. 7, the overlayer vibrations should be effectively decoupled from the collective modes of the substrate.

We remark that the kinetic energy (17.5 meV) of the He atoms used in the experiments[3] is comparable to the energies of the *z*-polarized modes Γ_2 and M_2, which implies a poor experimental resolution in this energy range. This could explain why such modes have not been ob-

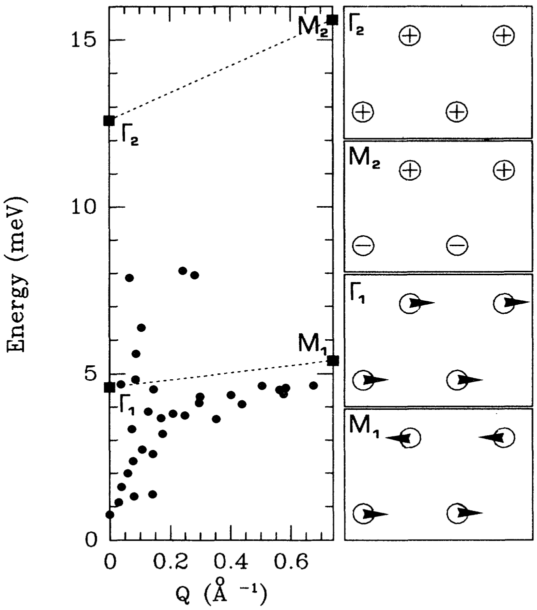

FIG. 7. Calculated phonon frequencies at the $\overline{\Gamma}$ and $\overline{M}$ points in the surface BZ of the (2×2) K overlayer. The displacement patterns used in our frozen-phonon calculations are shown schematically in the right part of the figure: crosses and minuses indicate atom displacement normal to the surface plane, arrows indicate displacements parallel to the surface. The dots are the experimental results of Ref. 3. The experimental points between 5 and 8 meV are believed to be overtones.

served with He scattering experiments. We finally note that, according to our calculations, the zone-center mode Γ_2 at ~ 13 meV is accompanied by a substantial macroscopic dipole moment perpendicular to the surface, corresponding to an effective charge $Z^* \sim 0.4e$, and thus should be easily observable using, e.g., electron-energy-loss spectroscopy (EELS) methods.

A detailed calculation of the phonon spectrum of the K-graphite system requires more sophisticated methods than the simple "frozen-phonon" approach used here. The *ab initio* molecular-dynamics (Car-Parrinello) method[24] has been used recently to study the phonon spectrum of a semiconductor surface.[42] In the present case, however, due to the very low frequencies of the overlayer vibrational modes, rather long simulation times $t_{\rm sim} > 1/\omega$ would be necessary, making this kind of approach prohibitively time consuming. The DF linear-response-theory approach of Ref. 41 would probably be the computational method of choice for accurate *ab initio* calculations of phonon dispersion curves in the system under study.

IV. SUMMARY

We have performed first-principles total-energy calculations to study the adsorption of potassium on graphite. The charge rearrangements which characterize the bonding of K to the substrate are analyzed and the details of K-graphite bonding, at two representative coverages, are elucidated. Our findings are in agreement with the experimental results of Ref. 5 in showing that the charge transfer is relevant but not complete in the low-coverage regime, whereas in the (2×2) overlayer phase, a lower charge transfer is accompanied by a vast redistribution of charge within the K monolayer.

The calculated surface corrugation of the (2×2) overlayer is found to be very small, in qualitative agreement with the He scattering results of Ref. 4. We find indications of a tendency of the substrate to reconstruct in the presence of K adatoms, although a more quantitative analysis requires additional, more converged calculations.

The unusual vibrational properties of the K-(2×2) overlayer are also investigated. The nearly dispersionless, low-energy mode observed at ~ 4 meV with inelastic He scattering[3] is attributed here to an in-plane vibration of the K monolayer. The existence at ~ 13 meV of a dipole-active mode of the overlayer polarized perpendicularly to the surface is predicted, which could be easily seen by EELS methods.

The results reported in this paper constitute a first step towards a deeper understanding of the alkali-metal–graphite interactions. Additional effort in first-principles calculations is, however, required in order to derive more quantitative results. In particular, the important issue of adatom-induced reconstruction of the graphite surface should be addressed in the future on a more quantitative basis.

ACKNOWLEDGMENTS

We thank I. Moullet and V. Celli for comments and advice. We thank M. W. Cole and R. D. Diehl for communicating to us the results of Refs. 4 and 3 prior to publication, and for useful discussions. We are grateful to P. Giannozzi for providing the pseudopotential for potassium used in our calculations. This work has been supported by the Italian Ministero della Pubblica Istruzione through the Consorzio Nazionale di Fisica della Materia, the Consiglio Nazionale delle Ricerche through Progetto Finalizzato "Sistemi Informatici e Calcolo Parallelo," and the National Science Foundation under Grant. No. DMR-9022681.

---

[1] For recent reviews on the argument, see *Physics and Chemistry of Alkali Metal Adsorption,* edited by H. P. Bonzel, A. M. Bradshaw, and G. Ertl (Elsevier, Amsterdam, 1989); T. Aruga and Y. Murata, Prog. Surf. Sci. **31**, 61 (1989).

[2] See, for instance, G. M. Lamble, R. S. Brooks, D. A. King, and D. Norman, Phys. Lett. **61**, 1112 (1988); S. A. Lindgren, C. Svensson, and L. Wallden, Phys. Rev. B **42**, 1467 (1990); M. Scheffler, Ch. Droste, A. Fleszar, F. Maca, G. Wachutka, and G. Barzel, Physica B **172**, 143 (1991); N. D. Lang, in *Physics and Chemistry of Alkali Metal Adsorption,* (Ref. 1); D. M. Riffe, G. K. Wertheim, and P. H. Citrin, Phys. Rev. Lett. **64**, 571 (1990); H. Ishida, Surf. Sci. **242**, 341 (1991); Phys. Rev. B **42**, 10 899 (1990); Z. Y. Li, K. M. Hock, and R. E. Palmer, Phys. Rev. Lett. **67**, 1562 (1991); A. Schmalz, A. Aminpirooz, L. Becker, J. Haase, J. Neugebauer, M. K. Scheffler, D. R. Batchelor, D. L. Adams, and E. Bogh, *ibid.* **67**, 2163 (1991).

[3] J. Cui, J. D. White, and R. D. Diehl (unpublished).

[4] J. Cui, J. D. White, R. D. Diehl, J. F. Annett, and M. W. Cole, Surf. Sci. **279**, 149 (1992).

[5] Z. Y. Li, K. M. Hock, and R. E. Palmer, Phys. Rev. Lett. **67**, 1562 (1991).

[6] Z. P. Hu, N. J. Wu, and A. Ignatiev, Phys. Rev. B **33**, 7683 (1986).

[7] M. T. Johnson, H. I. Starnberg, and H. P. Hughes, Surf. Sci. **178**, 290 (1986).

[8] N. J. Wu and A. Ignatiev, Solid State Commun. **46**, 59 (1983).

[9] N. J. Wu and A. Ignatiev, J. Vac. Sci. Technol. **20**, 896 (1982).

[10] H. Ishida and R. E. Palmer, Phys. Rev. B **46**, 15 484 (1992).

[11] E. Cheng, M. W. Cole, W. F. Saam, and J. Treiner, Phys. Rev. Lett. **67**, 1007 (1991).

[12] J. L. Martins and N. Troullier, Phys. Rev. B **46**, 1766 (1992).

[13] G. Galli, R. Martin, R. Car, and M. Parrinello, Phys. Rev. B **42**, 7470 (1990).

[14] S. Srivastava and J. Almlof, Surf. Sci. **274**, 113 (1992).

[15] S. B. Trickey, F. Muller-Plathe, G. H. F. Diercksen, and J. C. Boettger, Phys. Rev. B **45**, 4460 (1991).

[16] The presence of a non-negligible dipole at the K-graphite interface requires such a large region of vacuum in order to remove spurious effects due to the dipole-dipole interaction between the repeated images of the slab. We have verified that by increasing the vacuum region from ~ 18 a.u. to the value used in all our calculations, ~ 22 a.u., the total-energy variation is ~ 2 meV/atom, i.e., only $\sim 1\times10^{-5}$ of the total energy per atom.

[17] J. P. Perdew and A. Zunger, Phys. Rev. B **23**, 5048 (1981); D.

M. Ceperley and B. J. Alder, Phys. Rev. Lett. **45**, 566 (1980).

[18] G. B. Bachelet, D. R. Hamann, and M. Schluter, Phys. Rev. B **26**, 4199 (1982).

[19] L. Kleinman and D. M. Bylander, Phys. Rev. Lett. **48**, 1425 (1982).

[20] P. Giannozzi (unpublished).

[21] S. G. Louie, S. Froyen, and M. L. Cohen, Phys. Rev. B **26**, 1738 (1982).

[22] *CRC Handbook of Chemistry and Physics*, 67th ed. (CRC, Boca Raton, FL, 1986).

[23] M. Weinert, E. Wimmer, and A. J. Freeman, Phys. Rev. B **26**, 4571 (1982).

[24] R. Car and M. Parrinello, Phys. Rev. Lett. **55**, 2471 (1985); see also G. Galli and M. Parrinello, in *Computer Simulation in Material Science*, edited by M. Meyer and V. Pontikis (Kluwer, Dordrecht, 1991).

[25] F. Ganz, K. Staller, and J. Clark, Surf. Sci. **219**, 33 (1989).

[26] Z. P. Hu, J. Li, N. J. Wu, and A. Ignatiev, Phys. Rev. B **39**, 13 201 (1989).

[27] R. D. Diehl (private communication).

[28] The corresponding experimental value for the K binding energy in bulk phase is $E_b^{(\mathrm{K})} \sim 0.93$ eV per atom.

[29] M. Posternak, A. Baldereschi, A. J. Freeman, E. Wimmer, and M. Weinert, Phys. Rev. Lett. **50**, 761 (1983).

[30] J. K. Norskov, Phys. Rev. B **26**, 2875 (1982); N. D. Lang and J. K. Norskov, *ibid.* **27**, 4612 (1983); N. Esbjerg and J. K. Norskov, Phys. Rev. Lett. **45**, 807 (1980).

[31] M. W. Cole and F. Toigo, Phys. Rev. B **31**, 727 (1985).

[32] J. A. Barker and D. J. Auerbach, Surf. Sci. Rep. **4**, 1 (1984).

[33] J. A. Barker, N. Garcia, I. P. Batra, and M. Baumberger, Surf. Sci. **141**, L317 (1984).

[34] M. Manninen, J. K. Norskov, and C. Umrigar, Surf. Sci. **119**, L393 (1982).

[35] P. Cremaschi and J. L. Whitten, Surf. Sci. **169**, L289 (1986).

[36] E. Wimmer, H. Krakauer, M. Weinert, and A. J. Freeman, Phys. Rev. B **24**, 864 (1981).

[37] H. Zabel and A. Magerl, Phys. Rev. B **25**, 2463 (1982).

[38] R. Nicklow, N. Wakabayashi, and H. G. Smith, Phys. Rev. B **5**, 4951 (1972).

[39] E. de Rouffignac, G. P. Alldredge, and F. W. de Wette, Phys. Rev. B **23**, 4208 (1981).

[40] G. Benedek, G. Brusdeylins, C. Heimlich, J. P. Toennies, and U. Valbusa, Surf. Sci. **178**, 545 (1986).

[41] S. Baroni, P. Giannozzi, and A. Testa, Phys. Rev. Lett. **58**, 1861 (1987).

[42] F. Ancilotto, W. Andreoni, A. Selloni, R. Car, and M. Parrinello, Phys. Rev. Lett. **65**, 3148 (1990); F. Ancilotto, A. Selloni, W. Andreoni, S. Baroni, R. Car, and M. Parrinello, Phys. Rev. B **43**, 8930 (1991).